Photocatalytic Properties of SnO_2

Subjects: Others

Contributor: André L. Menezes de Oliveira , Mary Alves ,

SnO_2 is an n-type semiconductor with a band gap between 3.6 and 4.0 eV, whose intrinsic characteristics are responsible for its electrical conductivity, good optical characteristics, high thermal stability, and other qualities. Such characteristics have provided excellent results in advanced oxidative processes, i.e., heterogeneous photocatalysis applications. This process involves semiconductors in the production of hydroxyl radicals via activation by light absorption, and it is considered as an emerging and promising technology for domestic-industrial wastewater treatment.

tin oxide SnO2 synthesis method heterogeneous photocatalysis persistent organic pollutants POPs organic dyes

1. Tin-Oxide-Synthesis, Structure, Properties, and Applications as Heterogeneous Photocatalyst

Tin dioxide (SnO_2), obtained by combining Sn^{4+} and O^{2-}, is a ceramic material that has been used in a wide variety of applications, such as gas sensors, photovoltaic energy converters, and photocatalysts [1][2][3]. The success for multiple applications of SnO_2 is due to its intrinsic characteristics, such as: n-type conductivity, which is responsible for the conductivity of the material, and in addition to optical and electrical characteristics, high thermal stability, and high surface area [4][5][6]. Electrical conductivity can be described in terms of the movement of negatively charged electrons, and this gives rise to an n-type semiconductor [4][5][7][8][9].

As for the crystal structure of SnO_2, at room temperature, it adopts a rutile-type tetragonal structure (cassiterite) with *P42/mnm* space group, as illustrated in **Figure 1**. This structure is formed by a tetragonal unit cell defined by three (3) parameters: the *a* and *c* lattice parameters and the internal parameter, *u*, which defines the oxygen position (*u*, *u*, and 0). At room temperature, the theoretical lattice parameters for SnO_2 are a = 4.7374 Å, c = 3.1864 Å [10], and u = 0.3056 Å. It has been reported that SnO_2 can also adopt an orthorhombic, $CaCl_2$-type (*Pnnm*) structure, besides existing in an orthorhombic α-PbO_2-type (*Pbcn*), a cubic pyrite-type (*Pa*-3), an orthorhombic ZrO_2-type (*Pbca*), and a cotunnite-type (*Pnma*) structure. However, these structures are metastable at ambient conditions, and it is hard to follow these phase transitions through traditional methods under low pressure and temperatures [11][12].

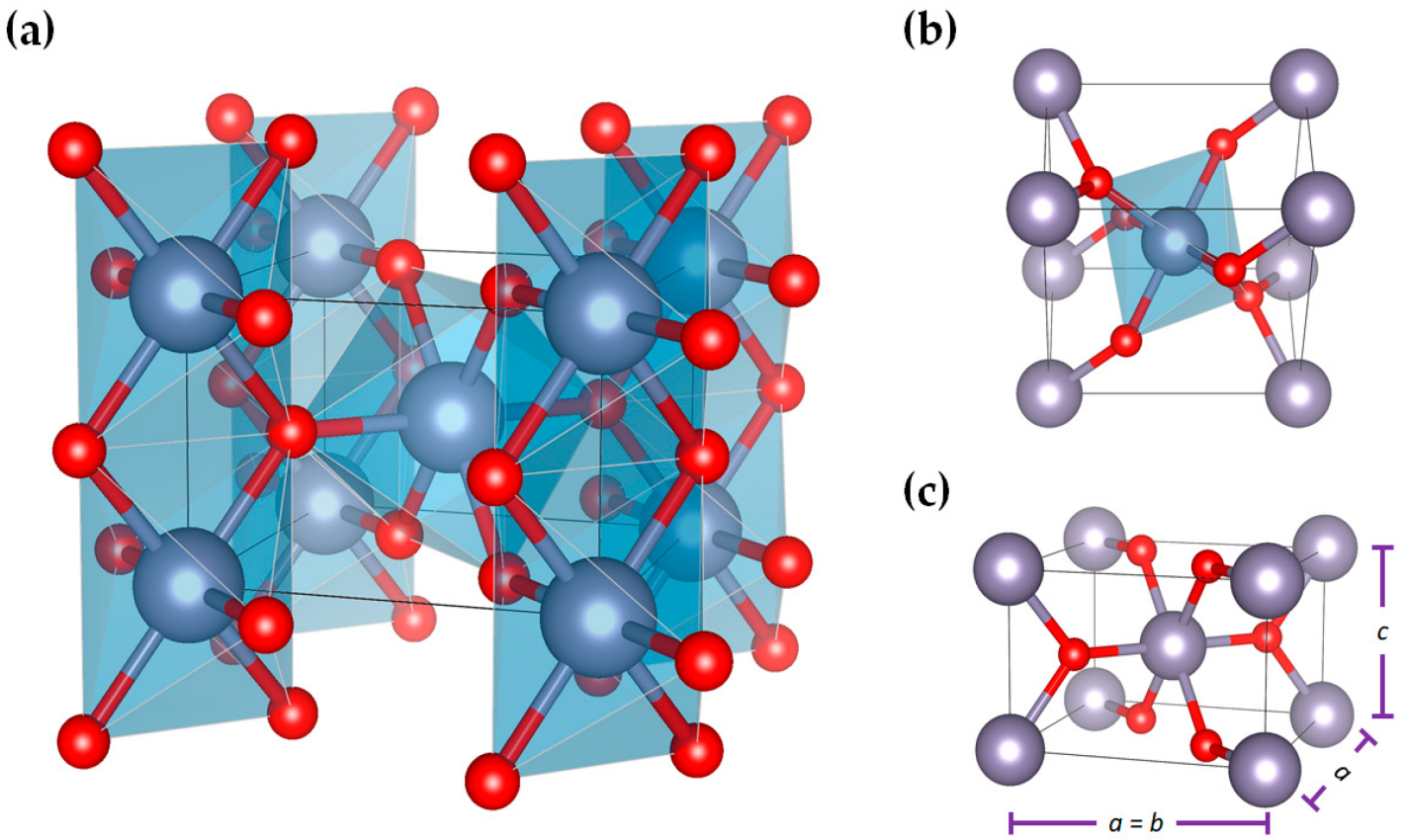

Figure 1. (**a**) A *P42/mnm* tetragonal crystal structure of SnO_2 showing (**b**) environment of distorted SnO_6 octahedron and (**c**) lattice parameters, obtained using VESTA software and structural parameters reported in [13].

The structure of SnO_2 consists of chains of SnO_6 octahedra in which each Sn atom is octahedral, surrounded by six oxygen atoms, while each oxygen is surrounded by three Sn atoms arranged at the corners of an equilateral triangle. The structure's Sn:O coordination is 6:3, with each octahedron not being regular, showing a slight orthorhombic distortion [10][13].

SnO_2 can present nano- and micro-structured characteristics, however, most researchers have been dedicated to the synthesis of SnO_2 in the form of nanoparticles. Such characteristics have offered good opportunities to explore new physical and chemical applications. Recently, SnO_2 has been applied to the degradation of antibiotics [14], fuel cell catalysts [13], gas sensors [15], sodium ion batteries [16], light-emitting diodes [17], heterogeneous photocatalysis, and antimicrobial activity [18][19]. There are several synthesis routes and experimental conditions to obtain SnO_2 in powder form, the choice of which may influence the particles' morphology and texture, besides their structural, optical, and electronic properties, which will consequently impact the efficiency and final application of the material. In relation to SnO_2-based thin films, chemical deposition methods have appeared to be the most used [20][21][22][23][24][25].

With respect to the applications in photocatalysis, SnO_2 catalysts with a tetragonal, rutile-type structure are the main phases investigated, but a recent work reported that the coexistence of mixed tetragonal–orthorhombic phases affected the photocatalytic efficiency of SnO_2 [26].

2. Synthesis Methods and the Influence of Experimental Parameters on the Characteristics and Photocatalytic Properties of SnO_2-Based Materials

One of the main aspects this entry refers to is the approach of how different synthesis methods and experimental parameters affect the photocatalytic properties of SnO_2-based materials.

Researchers have employed different methods to produce new materials with specific properties and applications. The choice of an appropriate condition to prepare a material is crucial to modifying its physicochemical characteristics, such as crystal structure and morphological and texture characteristics of the particles (size, shape, surface area, and surface charge characteristics), as well as the electronic and optical properties. The variation on these characteristics may change the applicability of the material. In this sense, different researchers have devoted to obtaining SnO_2-based materials with specific characteristics and efficient photocatalytic behaviors. Among the great variety of methods known in the literature, SnO_2-based photocatalysts have been obtained, in their powder form, by a solvothermal reaction [27][28], the microwave-assisted hydrothermal method [29], chemical precipitation [6], the polymeric precursor method [30], and sol-gel [31], all which are mostly used.

In relation to the photocatalytic properties of SnO_2 particles, although there is a variety of organic pollutants, organic dyes such as Methylene blue (MB), Rhodamine B (RhB), and Methyl orange (MO) have been the most used as target molecules to evaluate the photocatalytic efficiency of SnO_2. However, other organic dyes such as Congo red (CR), Malachite green (MG) and Eriochrome black T (EBT) have also been explored for such purposes. In this context, the photodegradation of these organic dyes is highlighted. Apart from powdered SnO_2 materials, SnO_2-based films have also been used as photocatalysts for dye photodegradation [32][33][34][35]. For the preparation of films, chemical [12][21][25][27][30] and physical-based deposition methods [12] are used. In the following sections, photocatalytic applications of pure and doped SnO_2-based catalysts, as well as the composites based on SnO_2 in powdered and film forms prepared by different techniques, are also discussed.

2.1. Pure SnO_2-Based Photocatalysts

Besides being synthesized in its pure form, SnO_2 has been prepared in its doped form with metals or nonmetal ions, as well as in the form of composites with other semiconductor materials, or even impregnated in inert, non-active photocatalytic materials. It is well known that the generation of electrons/holes (e^-/h^+) pairs by absorption of a photon of equal energy, to or higher than the band gap energy induced by light, is a basic prerequisite for a semiconductor to be used in photocatalysis. Because of its wide band gap of SnO_2 (3.6 eV), no absorption response to the visible light would be achieved, and this is the main disadvantage of this material, which restricts its application in practical devices. A wide variety of pure semiconductor materials, particularly SnO_2, have been investigated regarding the photocatalytic properties, but only few of them are considered effective photocatalysts.

Besides the value of the forbidden band energy corresponding to absorption in the visible region, it is required that the energy levels of the conduction and valence bands are suited to the redox potential of the water, so as to

produce reactive agents to promote breaking of organic pollutants molecules. Therefore, different authors have employed various synthesis methods and varied experimental conditions in order to change particle characteristics, which include size, morphology, and texture, as well as the crystallinity and the presence of defects, in order to design efficient photocatalysts under UV irradiation. These parameters can play an important role during photocatalysis, as they can affect the adsorptive and photo-absorption capacity of the catalyst, besides reducing photogenerated changes of recombination during photoexcitation. In addition, some authors also explored the reaction mechanisms involved in the photodegradation of the dyes and how the reactive species act for the photocatalysis to occur.

2.2. Doped SnO_2 Photocatalysts

Although pure SnO_2 nanoparticles with a different morphology have shown efficiency in the degradation of dyes under irradiation, different authors have developed strategies to overcome the low photoactivity of SnO_2 under visible light exposure. For instance, doping SnO_2 with different foreign ions has shown to be an efficient way to shorten its band gap and enhance its photoactivity.

Based on this fact, N. Mala et al. [36] synthesized SnO_2 nanoparticles doped with Mg^{2+} + Co^{3+} cations by a low-cost chemical solution method and investigated the antibacterial activity and photocatalytic efficiency toward the degradation of Methylene blue (MB) and Malachite green (MG) dyes. The authors revealed that the samples presented a tetragonal crystalline phase, with an average crystallite size of 24 and 25 nm for pure SnO_2 and SnO_2-Mg:Co, respectively. The authors suggested that this slightly increase of the crystallite size after doping was due to local distortions in the SnO_2 lattice induced by the presence of dopants. A nanorod-like morphology was confirmed through SEM images, with a reduction in the crystal length and in the average diameter after doping. Surprisingly, an increase in the band gap energy estimated for SnO_2 (3.52 eV) and SnO_2-Mg:Co (4.22 eV) was observed. This behavior is attributed to the quantum confinement effect that normally happens when the nanoparticle size decreases. However, no meaningful variation was observed in the particle size for pure and doped SnO_2 samples. Regarding the photocatalytic activity of SnO_2 and SnO_2:Mg:Co nanoparticles, the authors observed that SnO_2 presented an efficiency of 82 and 86%, while SnO_2-Mg:Co displayed 89 and 92% efficiency toward MB and MG dyes degradation, respectively, under visible light after 60 min.

Although doped SnO_2 is most prepared in powder, thin films based on doped SnO_2 have also been studied in photocatalysis. For instance, S. Vadivel and G. Rajaraja et al. [25] prepared magnesium-doped SnO_2 films by the chemical bath deposition method, varying Mg^{2+} molar concentrations (1, 5, and 10%). The films were deposited on glass, and after deposition they were annealed at 500 °C for 5 h in air to promote crystallization. From XRD analysis, the tetragonal rutile phase was confirmed in all films. Atomic force microscopy (AFM) images revealed that the surface roughness decreases with increasing dopant concentration. The optical band gap energy for pure SnO_2 was 3.63 eV, decreasing to 3.42 eV for the film doped with 10% Mg. The photocatalytic activities of the films were evaluated by the degradation of Methylene blue (MB) and Rhodamine B (RhB) dyes under UV irradiation. The maximum photodegradation of the dyes was reached for 10% Mg-doped SnO_2 film, degrading 80% of MB and

90% of RhB after 120 min. Fast electron transfer and high efficiency in electron–hole pairs separation led to a significant improvement of photocatalytic activity in the doped sample.

In the work conducted by Haya et al. [23] films of pure SnO_2 and doped with 2, 4, 6, and 8% of Sr^{2+} were prepared by a chemical solution deposition method using the sol-gel method to deposit the solution coating on a glass substrate. The effect of doping on the structural, optical, morphological, and photocatalytic properties of the films were studied. According to the results, the increase in Sr^{2+} doping promotes a decrease in crystallite size and an increase in the lattice distortion. These effects generate a greater number of defects, such as grain boundaries, micro-stresses, and displacements in the thin film lattice. The average crystallite size decreased from 7.61 nm for undoped SnO_2 to 3.80 nm for 8% Sr-SnO_2. It was also observed by UV-visible analysis that the presence of dopants introduced new intermediate levels in the semiconductor band gap (*Eg*), decreasing *Eg* from 3.86 eV for pure SnO_2 film to 3.76 eV for Sr-richer SnO_2 film. Additionally, the morphology of the films was analyzed by AFM, and a smaller grain size was observed for 8% Sr-SnO_2 (4.96 nm). Consequently, it showed the lower surface roughness when compared to the other films. Concerning the photocatalytic activity, the greatest efficiency in the degradation of MB dye under irradiation was attained for 8% Sr-SnO_2 film, which was attributed to smaller grain sizes and surface roughness, as well as the introduction of new energy levels below the conduction band of the pure material, resulting from the Sr doping.

Using a non-conventional method to prepare thin films, Loyola Poul Raj et al. [24] prepared SnO_2 thin films doped with 3 and 6 mol% of Tb^{3+} on a glass substrate by the spray nebulized pyrolysis (NSP) method and calcined them at 400 °C to crystallize the materials. The authors investigated the photocatalytic property of the films in the degradation of MB dye under UV irradiation. According to the authors, doping SnO_2 films with up to 6% of Tb^{3+} cations induces a decrease in the grain size from 80 to 56 nm, and the band gap from 3.51 to 3.36 eV, which directly impacts photocatalysis, as reported by other authors. Indeed, a maximum of 85% of dye degradation was observed after 120 min under UV irradiation using SnO_2 film doped with the 6 mol% Tb^{3+}. Using PL spectroscopy, the authors reveal that Tb doping leads to the creation of more defects that act as reactive sites for catalyzed reactions. As a consequence of the study, the authors concluded that Tb doping favored photocatalytic reactions by reducing particle size, and therefore increasing the surface area and the number of reactive sites on the surface, which allows the dye adsorption. In addition, Tb doping induces a decrease in the band gap of the materials, which favors photo-absorption, aiming to potentialize charge carriers to participate in photocatalytic reactions.

2.3. SnO_2-Based Composite Photocatalysts

As one can see from studies discussed in the sections above, pure and doped SnO_2 particles and films have been well explored. However, SnO_2 has also been combined with other different semiconductors in order to reduce recombination of the photoinduced charge carriers, to therefore improve photocatalytic activity.

Considering this fact, Abdel-Messih et al. [37] synthesized SnO_2/TiO_2 nanoparticles with a spherical mesoporous morphology synthesized by the sol-gel process, using polymethylmethacrylate as a template. The amount of SnO_2 (0–25%) in relation to the mass of pure TiO_2 was varied to obtain composites with different compositions. The

samples were calcined at 800 °C for 3 h to ensure complete organic polymer decomposition. In relation to the photocatalytic property of the materials, photodegradation of Rhodamine B (RhB) dye was performed under UV irradiation using a catalyst/dye concentration of 1 g L^{-1}. The photodegradation efficiency of the composites increased with the increase of tin oxide content up to 10% (about 92% of the dye degraded after 3 h). However, the sample with 25 mol% of SnO_2 showed the lowest efficiency, which was attributed to the loss of the titanium anatase phase. The authors concluded that there is an optimal amount of SnO_2 to achieve the maximum efficiency. In addition, the remarkable reduction in particle size by the existence of SnO_2 in the composites enhanced the oxidizing power and extended the photoinduced charge separation, and these were the main reasons for the increase in the catalytic activity of the samples.

2.4. Final Remarks

The number of materials for the formation of the SnO_2 with a different particle size and morphology, besides doped SnO_2 with an appropriate amount and type of dopant, and also the formation of the composite with SnO_2, plays an important role in improving the photocatalytic activity of the SnO_2 material. In relation to composites, the excess of both species can be harmful to the contact surface between the phases, mainly due to the high degree of particle agglomeration. Tests using scavengers, such as p-benzoquinone (BZ, $C_6H_4O_2$), isopropanol (ISO, $(CH_3)_2CHOH$), and ammonium oxalate monohydrate (AO, $(NH_4)_2C_2O_4{\cdot}H_2O$) indicate $^{\bullet}OH$ is the main species in most photocatalytic mechanisms. However, to obtain more insights about the photocatalytic mechanism involved in composite materials, the reseachers seek to understand the charge transfer between the phases from the band structures of each individual material. Structural and electronic defects can also generate energy levels between the VB and CB, and, therefore, modify the photocatalytic mechanism of composites. The creation of different interfaces between the phases may reduce charge carriers' recombination, leading to the formation of a great number of free radicals to improve photocatalysis. In addition, several other parameters can impact the photocatalytic efficiency of composites, such as phase composition, surface area, morphology, particle size, pore structure, electron–hole recombination rate, and band gap energy of the individual components. Some authors showed that the high surface area and the presence of pores are more effective parameters that affect dye degradation since the existence of several active sites, responsible for the adsorption of molecules, is crucial for the photocatalysis to occur.

Based on the findings above, it can be concluded that to design a new photocatalytic material with specific characteristic, one has to consider optimizing type and amount of dopants and interface characteristics between materials, or even the nature of the desired product (powder, film, etc.), besides the microstructure of the material (particle size and morphology), and by a choice of specific synthesis methodology and appropriate experimental conditions.

References

1. Lin, S.S.; Tsai, Y.; Bai, K. Structural and physical properties of tin oxide thin films for optoelectronic applications. Appl. Surf. Sci. 2016, 380, 203–209.
2. Feng, B.; Feng, Y.; Qin, J.; Wang, Z.; Zhang, Y.; Du, F.; Zhao, Y.; Wei, J. Self-template synthesis of spherical mesoporous tin dioxide from tin-polyphenol-formaldehyde polymers for conductometric ethanol gas sensing. Sens. Actuators B Chem. 2021, 341, 12995.
3. Noha, M.F.M.; Soha, M.F.; Tehb, C.H.; Lim, E.L.; Yap, C.C.; Ibrahima, M.A.; Ludina, N.A.; Teridi, M.A.M. Effect of temperature on the properties of SnO2 layer fabricated via AACVD and its application in photoelectrochemical cells and organic photovoltaic devices. Sol. Energy 2017, 158, 474–482.
4. Das, O.R.; Uddin, M.T.; Rahman, M.M.; Bhoumick, M.C. Highly active carbon supported Sn/SnO2 photocatalysts for degrading organic dyes. J. Phys. 2018, 1086, 012011.
5. Lavanya, N.; Fazio, E.; Neri, F.; Bonavita, A.; Leonardi, S.G.; Neri, G.; Sekar, C. Simulta neous electrochemical determination of epinephrine and uric acid in the presence of ascorbic acid using SnO2/graphene nanocomposite modified glassy carbon electrode. Sens. Actuators B Chem. 2015, 221, 1412–1422.
6. Das, M.; Roy, S. Preparation, Characterization and Properties of Newly Synthesized SnO2-Polycarbazole Nanocomposite via Room Temperature Solution Phase Synthesis Process. Mater. Today Proc. 2019, 18, 5438–5446.
7. Sakthiraj, K.; Balachandrakumar, K. Influence of Ti addition on the room temperature ferromagnetism of tin oxide (SnO2) nanocrystal. J. Magn. Magn. Mater. 2015, 395, 205–212.
8. Muthusamy, S.; Charles, J. In situ synthesis of ternary prussian blue, hierarchical SnO2 and polypyrrole by chemical oxidative polymerization and their sensing properties to volatile organic compounds. Optik 2021, 241, 166968.
9. Mallik, A.; Roy, I.; Chalapathi, D.; Narayana, C.; Das, T.D.; Bhattacharya, A.; Bera, S.; Bhattacharya, S.; De, S.; Das, B.; et al. Single step synthesis of reduced graphene oxide/SnO2 nanocomposites for potential optical and semiconductor applications. Mater. Sci. Eng. B 2021, 264, 114938.
10. Stöwe, K.; Weber, M. Niobium, tantalum, and tungsten doped tin dioxides as potentialn support materials for fuel cell cata-lyst applications. Z. Anorg. Allg. Chem. 2020, 646, 1470–1480.
11. Ono, S. High-pressure phase transitions in SnO2. J. Appl. Phys. 2005, 97, 073523.
12. Lian, Y.; Huang, X.; Yu, J.; Tang, T.B.; Zhang, W.; Gu, M. Characterization of scrutinyite SnO2 and investigation of the transformation with 119Sn NMR and complex impedance method. AIP Adv. 2018, 8, 125226.

13. Bolzan, A.A.; Fong, C.; Kennedy, B.; Howard, J.C. Structural Studies of Rutile-Type Metal Dioxides. Acta Crystallogr. B 1995, 53, 373–380.
14. Yang, C.; Fan, Y.; Li, P.; Gu, Q.; Li, X. Freestanding 3-dimensional macro-porous SnO2 electrodes for efficient electrochemical degradation of antibiotics in wastewater. Chem. Eng. J. 2021, 422, 130032.
15. Liu, B.; Li, K.; Luo, Y.; Gao, L.; Duan, G. Sulfur spillover driven by charge transfer between AuPd alloys and SnO2 allows high selectivity for dimethyl disulfide gas sensing. Chem. Eng. J. 2021, 420, 129881.
16. Qiua, H.; Zhenga, H.; Jin, Y.; Yuana, Q.; Zhanga, X.; Zhao, C.; Wangb, H.; Jia, M. Mesoporous cubic SnO2-CoO nanoparticles deposited on graphene as anode materials for sodium ion batteries. J. Alloys Compd. 2021, 874, 159967.
17. Kim, M.J.; Kim, T.G. Fabrication of Metal-Deposited Indium Tin Oxides: Its Applications to 385 nm Light-Emitting Diodes. Appl. Mater. Interfaces 2016, 8, 5453–5457.
18. Haq, S.; Rehman, W.; Waseem, M.; Shah, A.; Khan, A.R.; Rehman, M.; Ahmad, P.; Khan, B.; Ali, G. Green synthesis and characterization of tin dioxide nanoparticles for photocatalytic and antimicrobial studies. Mater. Res. Express 2020, 7, 025012.
19. Hojamberdiev, M.; Czech, B.; Goktas, A.C.; Yubuta, K.; Kadirova, Z.C. SnO2@ZnS photocatalyst with enhanced photocatalytic activity for the degradation of selected pharmaceuticals and personal care products in model wastewater. J. Alloys Compd. 2020, 827, 154339.
20. Kim, S.; Kwang, H.-K.C.; Kim, B.; Hyun-Jong, K.; Lee, H.-N.; Park, T.J.; Park, Y.M. Highly Porous SnO2/TiO2 Heterojunction Thin-Film Photocatalyst Using Gas-Flow Thermal Evaporation and Atomic Layer Deposition. Catalysts 2021, 11, 1144.
21. Bezzerrouk, M.A.; Bousmaha, M.; Akriche, A.; Kharroubi, B.; M'hamed, G. Hybrid structure comprised of SnO2, ZnO and Cu2S thin film semiconductors with controlled optoelectric and photocatalytic properties. Thin Solid Films 2013, 542, 31–37.
22. Han, K.; Peng, X.-L.; Li, F.; Yao, M.-M. SnO2 Composite Films for Enhanced Photocatalytic Activities. Catalysts 2018, 8, 453.
23. Haya, S.; Brahmia, O.; Halimi, O.; Sebais, M.; Boudine, B. Sol–gel synthesis of Sr-doped SnO2 thin films and their photocatalytic properties. Mater. Res. Express 2017, 4, 106406.
24. Raj, I.L.P.; Revathy, M.S.; Christy, A.J.; Chidhambaram, N.; Ganesh, V.; AlFaify, S. Study on the synergistic effect of terbium-doped SnO2 thin film photocatalysts for dye degradation. J. Nanopart. Res. 2020, 22, 359.
25. Va-divel, S.; Rajarajan, G. Effect of Mg doping on structural, optical and photocatalytic activity of SnO2 nanostructure thin films. J. Mater. Sci. Mater. Electron. 2015, 26, 3155–3162.

26. Li, Q.; Zhao, H.; Sun, H.; Zhao, X.; Fan, W. Doubling the photocatalytic performance of SnO2 by carbon coating mixed-phase particles. RSC Adv. 2018, 8, 30366–30373.
27. Hermawan, A.; Asakura, Y.; Inada, M.; Yin, S. One-step synthesis of micro-/mesoporous SnO2 spheres by solvothermal method for toluene gas sensor. Ceram. Int. 2019, 45, 15435–15444.
28. Hermawan, A.; Asakura, Y.; Inada, M.; Yin, S. A facile method for preparation of uniformly decorated-spherical SnO2 by CuO nanoparticles for highly responsive toluene detection at high temperature. J. Mater. Sci. Technol. 2020, 51, 119–129.
29. Wang, X.; Fan, H.; Ren, P.; Li, M. Homogeneous SnO2 core–shell microspheres: Microwave-assisted hydrothermal synthesis, morphology control and photocatalytic properties. Mater. Res. Bull. 2014, 50, 191–196.
30. Rodrigues, E.C.P.E.; Olivi, P. Preparation and characterization of Sb-doped SnO2 films with controlled stoichiometry from polymeric precursors. J. Phys. Chem. Solids 2003, 64, 1105–1112.
31. Varakina, Y.; Lahmanov, D.; Aksenov, A.; Trofimova, A.; Korobitsyna, R.; Belova, N.; Sobolev, N.; Kotsur, D.; Sorokina, T.; Grjibovsk, A.M.; et al. Concentrations of Persistent Organic Pollutants in Women's Serum in the European Arctic Russia. Toxics 2021, 9, 6.
32. Akram, M.; Saleh, A.T.; Ibrahim, W.A.W.; Awan, A.S.; Hussain, R. Continuous microwave flow synthesis (CMFS) of nano-sized tin oxide: Effect of precursor concentration. Ceram. Int. 2016, 42, 8613–8619.
33. Fatimah, I.; Purwiandono, G.; Jauhari, H.M.; Aisyah, A.A.; Sagadevan, P.; Oh, W.-C.; Doong, R.-A. Synthesis and control of the morphology of SnO2 nanoparticles via various concentrations of Tinospora cordifolia stem extract and reduction method. Arab. J. Chem. 2022, 15, 103738.
34. Abdelkader, E.; Nadjia, L.; Naceur, B.; Noureddine, B. SnO2 foam grain-shaped nanoparticles: Synthesis, characterization and UVA light induced photocatalysis. J. Alloys Compd. 2016, 679, 408–419.
35. Najjar, M.; Hosseini, H.A.; Masoudi, A.; Sabouri, Z.; Mostafapour, A.; Khatami, M.; Darroudi, M. Green chemical approach for the synthesis of SnO2 nanoparticles and its application in photocatalytic degradation of Eriochrome Black T dye. Optik 2021, 242, 167152.
36. Mala, N.; Ravichandran, K.; Pandiarajan, S.; Srinivasan, N.; Ravikumar, B.; Nithiyadevi, K. Enhanced antibacterial and photocatalytic activity of (Mg+Co) doped tin oxide nanopowders synthesised using wet chemical route. Mater. Technol. 2017, 32, 1328082.
37. Abdel-Messih, M.F.; Ahmed, M.A.; El-Sayed, A.S. Photocatalytic decolorization of Rhodamine B dye using novel mesoporous SnO2–TiO2 nano mixed oxides prepared by sol–gel method. J. Photochem. Photobiol. A Chem. 2013, 260, 1–8.